Nonlinear Kalman Filtering Techniques for Terrain-Aided Navigation

LARRY D. HOSTETLER, MEMBER, IEEE, AND RONALD D. ANDREAS

Abstract—**The application of nonlinear Kalman filtering techniques to the continuous updating of an inertial navigation system using individual radar terrain-clearance measurements has been investigated. During this investigation, three different approaches for handling the highly nonlinear terrain measurement function were developed and their performance was established. These were 1) a simple first-order extended Kalman filter using local derivatives of the terrain surface, 2) a modified stochastic linearization technique which adaptively fits a least squares plane to the terrain surface and treats the associated fit error as an additional noise source, 3) a parallel Kalman filter technique utilizing a bank of reduced-order filters that was especially important in applications with large initial position uncertainties. Theoretical and simulation results are presented.**

I. INTRODUCTION

SINCE the fundamental work of Kalman and Bucy [1], [2] in linear filtering theory, the application of Kalman filters for "optimally" updating navigation systems utilizing auxiliary-sensor data has received considerable attention. Among the navigation systems and aides that have been considered are star trackers, satellite positional fixes, visual positional fixes, landmark trackers, Doppler radars, Omega fixes, VOR/DME data, MICRAD fixes, and air dead-reckoning data [3]–[11].

Investigations are currently being conducted on the updating of inertial navigation systems (INS's) using positional fixes derived from optical, radiometric, or radar obtained terrain data. One of the more successful concepts to date has been the terrain contour matching (TERCOM) system being developed for cruise missile applications [12]–[14]. It basically provides a positional fix by correlating a radar-altimeter-derived terrain profile with a stored topographical map, taking the location of the best match to be the position of the navigator. A sequence of such positional fixes are then utilized as measurements for Kalman updating the position, velocity, and other modeled states in an INS. Although a Kalman filter is eventually utilized, TERCOM, as well as various other approaches to terrain guidance, is still essentially a correlation guidance scheme, i.e., the fundamental measurement utilized as input to the Kalman filter is a positional fix derived from a correlation/matching algorithm on the raw terrain-clearance data.

Manuscript received March 11, 1982; revised September 27, 1982. This work was supported by the U.S. Department of Energy.

The authors are with Sandia National Laboratories, Albuquerque, NM 87115.

A significantly different approach to terrain-aided navigation is the subject of this paper. In contrast to Kalman processing of derived positional fixes, this approach recursively treats each radar terrain-clearance measurement as the measurement to be Kalman processed. By viewing each radar terrain-clearance measurement separately, a new class of "continuously" terrain-aided navigation schemes becomes available that in the past could not easily be developed using correlation type methods. This new class has several significant system features. First, the ability to model significant INS and measurement errors allows the designer to approach optimum accuracy and to desensitize the system to error sources that might otherwise compromise the updating process. Second, updating can occur continuously to a target because the recursive algorithms are not complicated by vehicle maneuvers. Third, the standard practices of covariance analysis inherent in the Kalman technique offer, with appropriate interpretation, an approach to predicting system performance and performing tradeoff studies during preliminary design. And finally, systems in which the error sources do not permit simple correlations algorithms to be derived, e.g., highly inaccurate INS's containing large velocity, attitude, accelerometer and gyro errors, air dead-reckoning and Doppler navigation systems, etc., can now be optimally aided using terrain data.

A program of concept development and flight test evaluation of terrain-aided navigation has been pursued at Sandia National Laboratories since 1974 [15], [23]. This program concentrated on an application with a radar altimeter operating at low altitude, an inertial navigation system, and updating occurring over distances of 40 km or less. Other applications and navigational systems have also been studied, but the important theoretical as well as practical problems are embodied in this setting.

Due to the undulating nature of terrain, the radar terrain-clearance measurement is a nonlinear function of vehicle position. Thus, the basic theory required for optimally processing these measurements is that of nonlinear estimation theory and its approximations [24], [25]. In addition, since the terrain beneath the vehicle is constantly changing, the nonlinearities are functions of time. Properly accounting for these nonlinearities is essential in obtaining satisfactory performance.

The following sections first give the general framework for optimal terrain-aided navigation systems. They then

0018-9286/83/0300-0315$01.00

address several specific system configurations that involve different methods for treating measurement nonlinearities. Included are performance comparisons and discussions of the limitations of each method.

II. Nonlinear Kalman Filter Framework

The basic configuration for optimal terrain-aided navigation is shown in Fig. 1.

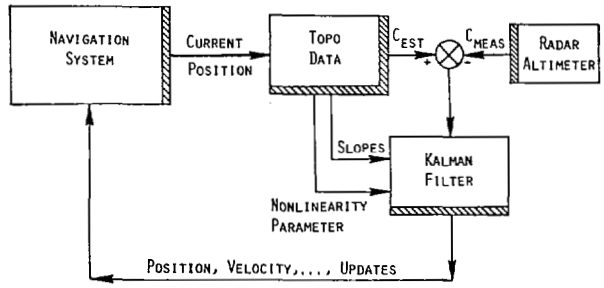

Fig. 1. Optimal terrain-aided navigation.

This structure is typical of Kalman filtering in which nonlinear auxiliary measurements are iteratively processed to estimate and compensate for the errors in a navigation system. At each measurement update time the current state estimate, in conjunction with stored topographical data, is used to obtain a prediction of what the radar ground clearance measurement should be. The actual radar measurement is then compared with this predicted measurement, and their difference is processed by the Kalman filter to generate estimates of the navigation system's error states. The measurement matrix in this case is related to the downrange and crossrange terrain slopes calculated from the stored data. The error estimates are then fed back to compensate the navigation system and thus provide an improved estimate of the actual state (position, velocity, etc.) of the system. This process is iterated many times, e.g., every 30–50 m of distance traveled, as the system maneuvers along its trajectory, thus providing essentially continuous updating to the navigation system.

In order to apply approximate nonlinear filtering algorithms, a set of differential equations describing how the states of the navigation system propagate is required. It is sufficient here to assume the following general form of system model [24], [25]:

$$\dot{x}(t) = f(x(t), t) + w(t) \tag{1}$$

where $x(t)$ is the vector of states in the navigation system and $w(t)$ is the Gaussian system noise vector with $E\{w(t)\} = \mathbf{0}$ and

$$E\{w(t)w^T(t+\tau)\} = Q(t)\delta(\tau).$$

The state estimate propagation equation[1] between terrain-clearance measurements is

$$\dot{\hat{x}}(t) = f(\hat{x}(t), t) \tag{2}$$

and the error covariance propagation equation[1] is

$$\dot{P}(t) = F(\hat{x}(t), t)P(t) + P(t)F^T(\hat{x}(t), t) + Q(t) \tag{3}$$

where the $\hat{}$ notation refers to an estimate and F is the partial derivative matrix of f with respect to x. The emphasis here is on the use of nonlinear *measurements*. The state dynamics are assumed to be a very good linear approximation. Actually, in practice the position and other necessary errors are included in the state vector and constantly updated in the navigational system to maintain the adequacy of such a representation.

The terrain-clearance measurement equation is in general a nonlinear function of the antenna pattern, the crossrange/downrange position (CR, DR), altitude (z), and attitude (ψ) of the vehicle. In most instances,[2] a reasonable approximation to the kth terrain-clearance measurement is

$$\begin{aligned} c_k &= c_k(x_k) + v_k \\ &= z_k - h(CR_k, DR_k) + v_k \end{aligned} \tag{4}$$

where $h(CR, DR)$ is the height of the terrain at the position (CR, DR), and v_k is the measurement error with $E\{v_k\} = 0$ and $E\{v_k v_j\} = r_k \delta_{kj}$. The measurement error consists of both radar altimeter error and reference map errors. If these errors are correlated processes it may be necessary to model them as such.

Following the derivation in Gelb [25, ch. 6], when the measurement c_k is taken, the measurement update equations are given by

$$\hat{x}_k(+) = \hat{x}_k(-) + K_k[c_k - \hat{c}_k(x_k)] \tag{5}$$

where $\hat{x}_k(+)$ is the estimate after updating, $\hat{x}(-)$ is the estimate prior to the update, and $\hat{c}_k(x_k) \triangleq E\{c_k(x_k)\}$ is the predicted clearance measurement, where we will now approximate the expectation by assuming x_k is Gaussian with mean $\hat{x}_k(-)$ and covariance matrix $P_k(-)$. The optimal gain matrix is given by

$$\begin{aligned} K_k = E\{[x_k - \hat{x}_k(-)][c_k(x_k) - \hat{c}_k(x_k)]^T\} \\ \cdot \left[E\{[c_k(x_k) - \hat{c}_k(x_k)][c_k(x_k) - \hat{c}_k(x_k)]^T\} + r_k\right]^{-1}. \end{aligned} \tag{6}$$

And, finally, the error covariance measurement update equation is given by

$$\begin{aligned} P_k(+) = P_k(-) - K_k E\{[c_k(x_k) - \hat{c}_k(x_k)] \\ \cdot [x_k - \hat{x}_k(-)]^T\}. \end{aligned} \tag{7}$$

The techniques utilized in the implementation and evaluation of these equations and expectations are funda-

[1] These are the first-order appropriations [25] to the more general nonlinear expressions for propagating the conditional mean and its associated covariance matrix

$$P(t) = E\{[\hat{x}(t) - x(t)][\hat{x}(t) - x(t)]^T\}.$$

[2] For cases where the radar altimeter tracks a "closest point" that is not near nadir, the measurement function needs to account for the nonlinear variation with altitude z_k as well as the usual variation with downrange and crossrange positions.

mental in obtaining satisfactory terrain-aided performance, i.e., avoiding divergent filter behavior while maintaining highly accurate state position estimates.

In particular, satisfactory performance depends upon the adequacy of the basic approach used to linearize the measurement function in the calculation of (6) and (7), i.e., to linearize the terrain. Since the expectations must be taken with respect to the current state estimate uncertainties, whatever linearization is used must be valid over a region whose size is consistent with current position estimation errors.

If the position errors are sufficiently small relative to the terrain correlation length, it can be assumed that the terrain is linear and simple first-order spatial derivatives will yield satisfactory performance. In cases where position errors are comparable to or larger than the terrain correlation length, more sophisticated linearization techniques are required.

Three different linearization approaches for treating terrain nonlinearities are discussed in the following sections. The first two, local slope linearization and stochastic linearization, attempt to maintain satisfactory performance within a single Kalman filter framework. The third approach utilizes parallel Kalman filters, each linearized over a different region to handle the case of very large (relative to the terrain correlation length) initial position errors.

III. Local Slope Linearization

The standard extended Kalman approach to linearization is to expand a nonlinear measurement function in a Taylor series about the current state estimates, retain the linear terms, and neglect higher order ones. With the definition of $c_k(\boldsymbol{x}_k)$ from (4), the predicted clearance measurement approximation becomes

$$\hat{c}_k(\boldsymbol{x}_k) = \hat{z}_k(-) - h\big(\widehat{CR}_k(-), \widehat{DR}_k(-)\big) = c_k(\hat{\boldsymbol{x}}_k) \quad (8)$$

and the linearization becomes

$$c_k(\boldsymbol{x}_k) \triangleq c_k(\hat{\boldsymbol{x}}_k) + H_k\big[\boldsymbol{x}_k - \hat{\boldsymbol{x}}_k(-)\big] \quad (9)$$

where the measurement matrix H_k is defined by

$$H_k = [-\text{crossrange slope}, -\text{downrange slope}, 1, 0, 0, \cdots] \quad (10)$$

with the first three states being taken to be crossrange (CR), downrange (DR), and altitude (z), respectively.

Substituting (9) and (10) into (5), (6), and (7) yields the following standard extended Kalman filter update equations [25]:

$$\hat{\boldsymbol{x}}_k(+) = \hat{\boldsymbol{x}}_k(-) + K_k\big[c_k - c_k(\hat{\boldsymbol{x}}_k)\big], \quad (11)$$

$$P_k(+) = \big[I - K_k H_k\big] P_k(-), \quad (12)$$

and

$$K_k = P_k(-) H_k^T \big[H_k P_k(-) H_k^T + r_k\big]^{-1}. \quad (13)$$

To demonstrate the performance of the standard extended Kalman filter equation, a Monte Carlo simulation

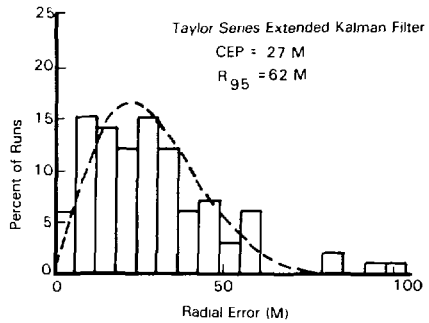

Fig. 2. Standard extended Kalman filter performance.

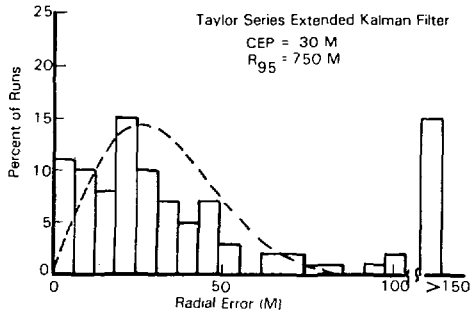

Fig. 3. Standard extended Kalman filter divergence problem.

of the above equations was performed. A short-range standoff mission scenario was utilized with the system navigating from an initialization point (IP) to a target located approximately 6 km away. The flight time and speed were approximately 40 s and 150 m/s, respectively. A low altitude flight profile was assumed with radar altimeter measurements being processed every 0.4 s. The measurement noise was assumed to be 6 m. Finally, the inertial system errors were modeled for this short mission as being adequately represented by three position and three velocity error states. The initial velocity error standard deviations were taken to be approximately 3 m/s in the east and north states and 0.3 m/s in the vertical state. The initial position error standard deviations were 15 m in all three position error states. The terrain consisted of rolling hills having a terrain height standard deviation (σ_T) of approximately 12 m, a correlation length near 500 m, and a slope standard deviation near 5 percent. Fig. 2 shows the histogram of radial misses at the target for 100 Monte Carlo runs.

As seen, the filter achieved a 27 m circular error probable (CEP) at the target. This is a significant improvement over the unaided inertial system which would have had a 120 m CEP due to its large velocity errors. The dashed curve is a theoretical Rayleigh distribution also having a 27 m CEP.

Unfortunately, as mentioned earlier, the highly nonlinear nature of terrain surfaces can lead to filter divergence, especially when the linearization error is comparable to the measurement error. In these cases the standard extended Kalman filter may yield unsatisfactory performance, and divergence can occur in which the actual estimation errors become orders of magnitude larger than the filter's own computation of their covariance [26]. Fig. 3 demonstrates

this phenomenon for a simulation test case in which the initial position error standard deviations were 75 m and all other conditions were the same as in the prior simulation. Note that the error distribution is quite non-Rayleigh and has an unexpectedly long tail (more than 15 percent of the Monte Carlo runs had target errors greater than 150 m). This divergence problem is severe, and when it occurs the errors become catastrophic as indicated by a 95th percentile of 750 m for the radial misses. A solution to this problem is the subject of the following section.

IV. Modified Stochastic Linearization

Techniques for obtaining approximate nonlinear filters that attempt to account for measurement nonlinearities and prevent filter divergence have been investigated [24], [25]. This section describes an extension of these techniques and the subsequent application of them to our terrain-aided navigation problem.

Define the stochastic linearization of $c_k(\boldsymbol{x}_k)$ by

$$c_k(\boldsymbol{x}_k) \triangleq \hat{c}_k(\boldsymbol{x}_k) + H_k\left[\boldsymbol{x}_k - \hat{\boldsymbol{x}}_k(-)\right] + \epsilon_{\text{fit}} \tag{14}$$

where $\hat{c}_k(\boldsymbol{x}_k) \triangleq E\{c_k(\boldsymbol{x}_k)\}$ is as previously defined, ϵ_{fit} is the linearization fit error, and the measurement matrix H_k is redefined by

$$H_k \triangleq E\left\{\left[c_k(\boldsymbol{x}_k) - \hat{c}_k(\boldsymbol{x}_k)\right]\left[\boldsymbol{x}_k - \hat{\boldsymbol{x}}_k(-)\right]^T\right\} P_k^{-1}(-). \tag{15}$$

From the definition of $\hat{c}_k(x_k)$ and H_k, and since we are assuming $\boldsymbol{x}_k$ to be Gaussian with mean $\hat{\boldsymbol{x}}_k(-)$ and covariance $P_k(-)$, one sees that they are simply the least square linear approximation of $c_k(\boldsymbol{x}_k)$ about $\hat{\boldsymbol{x}}_k(-)$ using a Gaussian weighing function with covariance $P_k(-)$.

Making the simplifying approximation that the fit error is uncorrelated with $c_k(\boldsymbol{x}_k)$ and $H_k[\boldsymbol{x} - \hat{\boldsymbol{x}}_k(-)]$ and substituting (14) and (15) into (5), (6), and (7) yields the following measurement update equations:

$$\hat{\boldsymbol{x}}_k(+) = \hat{\boldsymbol{x}}_k(-) + K_k\left[c_k - \hat{c}_k(\boldsymbol{x}_k)\right] \tag{16}$$

$$P_k(+) = \left[I - K_k H_k\right] P_k(-) \tag{17}$$

and

$$K_k = P_k(-) H_k^T \left[H_k P_k(-) H_k^T + r_k + r\text{fit}_k\right]^{-1} \tag{18}$$

where $r\text{fit}_k \triangleq E\{\epsilon_{\text{fit}}\epsilon_{\text{fit}}^T\}$ is the variance of the fit error due to the nonlinearity of the terrain. Note that the usual stochastic linearization equations [25] have been modified by the inclusion of the fit error variance. This additional term is very important in that, similar to second-order techniques, [26], the increased variance keeps the Kalman filter from utilizing data from regions of high nonlinearity. Since this term varies with time, as the terrain nonlinearities vary, the filter will emphasize those measurements with less linearization fit error. For typical terrain, the fit error can be quite large at times relative to the usual measurement noise. In addition, the fit errors are often large in regions of terrain having steep slopes. Thus, without the additional fit error being considered, the usual stochastically linearized filter would place the most weight on measurements which violated the linearity assumption the worst, obviously not a desirable situation.

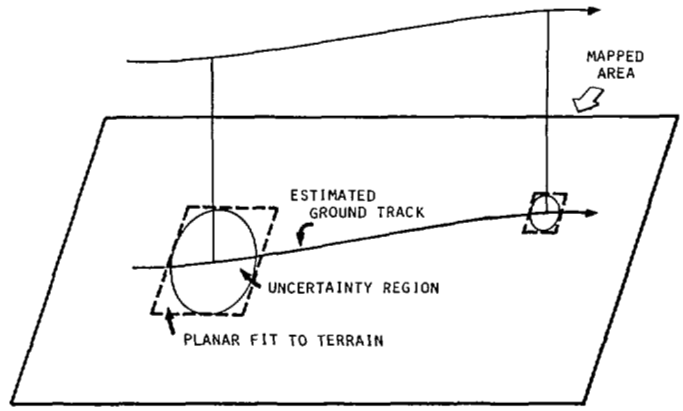

Fig. 4. Modified terrain linearization process.

Since the linearization is being done using the current covariance estimate $P_k(-)$, the size of the region of linearization is proportional to the position uncertainty at that point. Thus, the technique is adaptive and, assuming large initial position uncertainty, tends to initially smooth out the terrain and its slope variations. However, as the CEP improves and the position uncertainty reduces in size, the smoothing is lessened, the fit error decreases, and the filter is able to take advantage of the higher frequency content in the terrain to further decrease its CEP. This concept is illustrated in Fig. 4.

With the definition of $c_k(\boldsymbol{x}_k)$ from (4),

$$\hat{c}_k(\boldsymbol{x}_k) = \hat{z}_k(-) - \hat{h}(CR_k, DR_k), \tag{19}$$

and treating the terrain height as a function of position only, H_k becomes

$$H_k = \left(-H_{CR_k}, -H_{DR_k}, 1, 0, \cdots\right) \tag{20}$$

where the first three states are taken to be crossrange (CR), downrange (DR), and altitude (z), respectively. $\hat{h}(CR_k, DR_k)$, H_{CR_k}, and H_{DR_k} are the parameters of the least square linear approximation of the terrain $h(CR, DR)$ about $\widehat{CR}_k(-)$ and $\widehat{DR}_k(-)$ using the Gaussian covariance matrix corresponding to the CR and DR part of $P_k(-)$.

Fig. 5 illustrates how certain problems are avoided by this modified stochastic linearization technique. For position uncertainties that are large relative to the nonlinearities in the terrain, the simple Taylor series expansions used in both the usual extended Kalman and second-order Gaussian filters can lead to large measurement and linearization slope errors. These errors can quickly lead to filter divergence. Also shown is the fit error due to the nonlinear terrain. It is easy to see that the variance of this error ($r\text{fit}$) will vary with time and, in general, will decrease as the position error decreases. In addition, as the position error

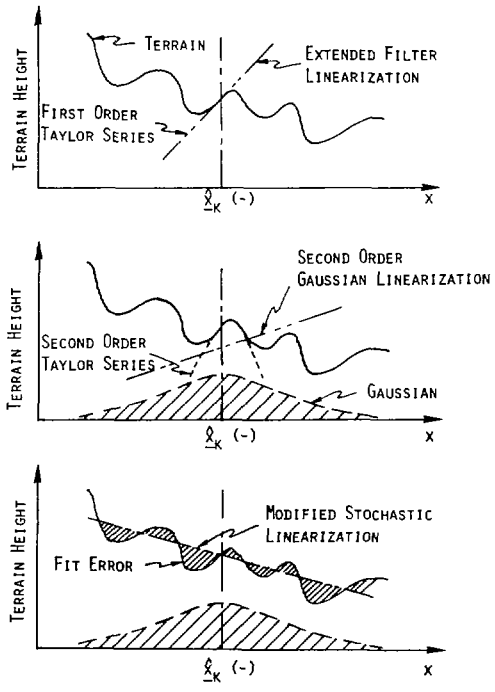

Fig. 5. Linearization techniques.

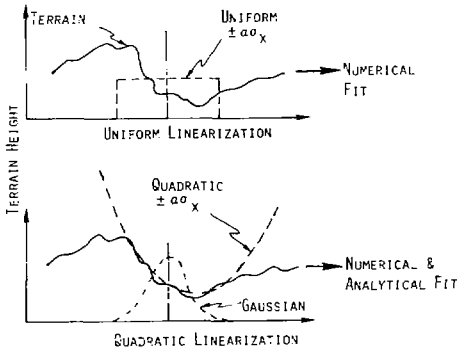

Fig. 6. Modified stochastic linearization.

decreases, the linearization slopes increase. These two effects work together to allow the filter to effectively use the low frequencies in the terrain at first, but to converge and take advantage of the higher frequencies as the system updating proceeds. In the limit as the position errors decrease, the terrain becomes locally linear and the stochastic linearization becomes equivalent to the extended and second-order filter linearizations.

The actual stochastic linearization utilizes the stored topographical data. A straightforward least squares fitting of a plane to the gridded data can be carried out using, as the weighting function, a Gaussian density centered at the current state estimate and having as its covariance matrix the current position error covariance. The variance of the weighted residuals is $r\text{fit}_k$. Two other techniques for approximating this calculation are shown in Fig. 6.

The uniform stochastic linearization essentially approximates the Gaussian weighting function by a uniform density over a region whose size and shape is proportional to the current position uncertainty. Ordinary least squares

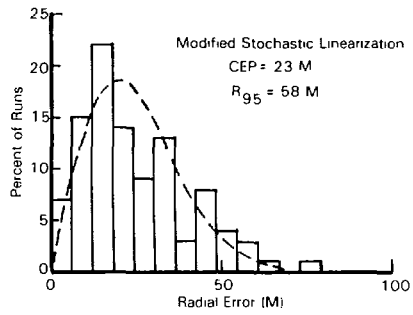

Fig. 7. Performance improvement with modified stochastic linearization.

equations for the plane and residual error result. This is the technique used for the simulations in the following section.

The quadratic stochastic linearization essentially approximates the terrain as a quadratic surface over a region proportional to the current position uncertainty and then analytically linearizes this quadratic surface using a Gaussian weighting function. The fit variance ($r\text{fit}_k$) in this case is the sum of the numerically calculated quadratic residual error plus an additional amount due to the subsequent analytical linearization of the quadratic surface.

It should be noted that if there is significant noise in the stored reference data, lower bounds should be placed on the size of the fit regions. This guarantees that the reference errors will not adversely affect the slope calculations.

The above basically describes the modified stochastic linearization technique used for optimally processing the terrain-clearance data. The authors feel that this modified technique should find applications in other nonlinear filtering problems and should provide superior performance over both the usual second-order Gaussian filter as well as the standard stochastically linearized filter when the measurement equation is highly nonlinear. Finally, the consideration of errors in ones knowledge of the actual measurement function and the techniques for handling these errors contribute to preventing filter divergence.

V. Modified Stochastic Linearization Performance

As shown earlier in Fig. 3, the local slope linearization approach can lead to filter divergence under certain conditions. To demonstrate the improved performance of the modified stochastic linearization technique, the same case was simulated using the new approach. Fig. 7 demonstrates the improved performance, where the divergence problem disappeared, and accuracy improved as well. Again, the dashed curve is the Rayleigh density function having the same CEP as the histogram.

System accuracy in general is a function of INS errors, measurement errors, and terrain signature levels. Considerable insight into filter performance and into those parameters influencing system accuracy can be gained through closed-form analytical approximations of predicted performance. Utilizing standard estimation theory techniques, subject to some reasonable limitations on ter-

rain roughness and update interval size, general expressions for filter performance have been derived. For example, if the inertial system is modeled as having only position errors in all three axes, the estimation error covariance matrix $\boldsymbol{P}$ for downrange and crossrange positions is given by

$$\boldsymbol{P} = \begin{bmatrix} \frac{1}{\sigma_{sdr}^2} & \frac{\rho}{\sigma_{sdr}\sigma_{scr}} \\ \frac{\rho}{\sigma_{sdr}\sigma_{scr}} & \frac{1}{\sigma_{scr}^2} \end{bmatrix} \cdot \frac{\sigma_n^2}{\sqrt{N\cdot(1-\rho^2)}} \tag{21}$$

where

$\sigma_{sdr}, \sigma_{scr}$ = downrange and crossrange terrain slope standard deviations computed from the terrain slope history obtained by terrain linearization.

ρ = correlation between downrange and crossrange slopes from the terrain slope history.

σ_n = measurement noise standard deviation.

N = number of independent measurements.

Note that this covariance matrix has the property of including the terrain roughness variations and correlations between the crossrange and downrange directions and that the error covariances are proportional to the variance of the measurement errors. Performance characterization can be further simplified as this equation describes the covariance of a bivariate Gaussian density function. If the terrain has uncorrelated slopes in the downrange and crossrange directions with equal slope standard deviations, CEP can be expressed as

$$\text{CEP} = \frac{1.17\sigma_n}{\sqrt{N}\,\sigma_s} \tag{22}$$

where $\sigma_s = \sigma_{sdr} = \sigma_{scr}$. Similar position error and velocity error predictions are obtainable for the case when velocity errors are also present in the inertial system and must be estimated. These are

$$\text{CEP}_p = \frac{2.35}{\sqrt{N}}\frac{\sigma_n}{\sigma_s}, \tag{23}$$

$$\text{CEP}_v = \frac{4.08}{\sqrt{N}}\frac{\sigma_n}{T\sigma_s} \tag{24}$$

where

CEP_p = position CEP,

CEP_v = velocity CEP,

T = total flight time.

As indicated, the terrain roughness parameter characterizing performance is the standard deviation of the terrain slopes evaluated along the reference trajectory. Assuming a total flight time of 40 s incorporating 100 independent updates, Fig. 8 shows predicted performance (23) as a function of terrain roughness for several values of measurement noise. For reference, a σ_s of 0.02 is typical of terrain with a standard deviation of 5 m. The simulation results shown in Figs. 2 and 7 basically agree with these curves.

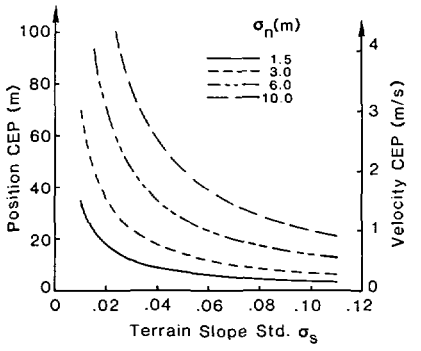

Fig. 8. System performance.

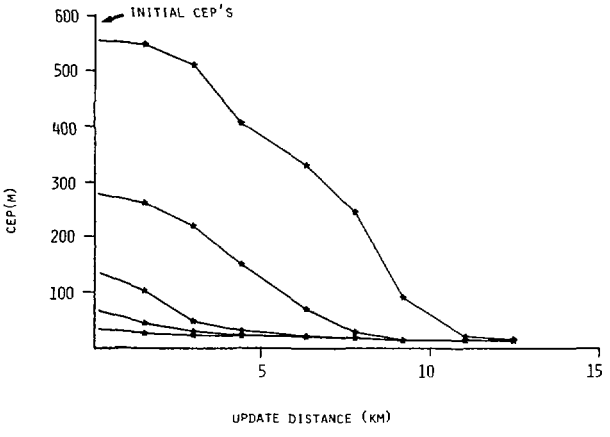

Fig. 9. Terrain smoothing effect on performance.

Because of the time varying nature of both the terrain slopes and the corresponding measurement errors, additional insight and performance and error sensitivity analyses can be obtained through covariance propagation techniques [25]. The general approach is to utilize a terrain slope history (downrange and crossrange) derived from actual topographical data and process it in a covariance analysis computer program to predict performance for any candidate filter design. This procedure was used to generate Fig. 9, which plots CEP histories for various initial position uncertainties. All other conditions were as before and again 6 m of measurement noise was assumed here. These data were calculated by propagating covariances using stochastic linearization along a particular trajectory over the prior mentioned terrain. Note that although the system eventually achieves equivalent accuracy independent of initial CEP, the required flight path is considerably longer for the larger starting CEP's. Thus, the basic effect of stochastic linearization is to smooth or low-pass filter the reference topography so that the calculated terrain slopes are the average slopes over the current position

uncertainty region. When the initial position uncertainties are large compared to the terrain correlation length, the resulting terrain smoothing can become excessive. Hence, this method of terrain linearization is clearly restrictive in applications where initial CEP is large and the update distance is limited.

It should be noted here that if batch processing were allowed, this restriction could possibly be overcome by a globally iterated filter-smoother [24] iteratively sweeping through the data, utilizng the state estimate and improved CEP of each previous sweep as the starting point until no further improvement was warranted. This procedure would prevent divergence due to large initialization errors while at the same time allowing for eventual utilization of the full frequency content of the terrain and the correspondingly smaller CEP. This approach not only requires storage of INS and altimeter measurements, but is nonreal-time and is not appropriate for some applications.

Fortunately, a parallel filter structure approach has been developed for handling this delayed convergence problem and is the subject of the next section.

VI. Parallel Filter Structure

The approach developed to handle the case of large initial errors is embodied in the processing approach shown in Fig. 10 where a bank of parallel filters[3] and a set of position displaced INS trajectories are employed [21]–[23]. Each of the parallel filters linearizes around and generates error estimates for its trajectory. Therefore, the operation of each filter can be viewed as altering its trajectory within the degrees of freedom allowed by the number of modeled states to achieve the best match of the measuremens with the terrain in the vicinity of its trajectory. A selection algorithm can then be used that examines the residuals of each filter to select which filter has the best match, i.e., is using the proper terrain and whose error estimates have converged. Note that for a given initial CEP, the number of filters, and hence filter spacing can be adjusted so that the starting uncertainty for each filter is as small as desired. Note also that after an appropriate distance has been flown, the parallel structure would no longer be needed and one filter would be sufficient for continued system operation.

The selection of the convergent filter can be done quite easily by examining the residuals Δ_i for each filter. A selection algorithm based upon the assumed whiteness property of the filter residuals that worked well in practice is to choose the filter with the smallest value of

$$\text{AWRS}_{j\text{th filter}} = \frac{1}{N}\left[\sum_{i=1}^{N} \frac{\Delta_i}{H_i P_i H_i^T + R_i}\right]_{j\text{th filter}} \tag{25}$$

[3] The parallel filter structure discussed here is part of a very broad class of algorithms which has come to be referred to as multiple model estimation algorithms [27]–[29].

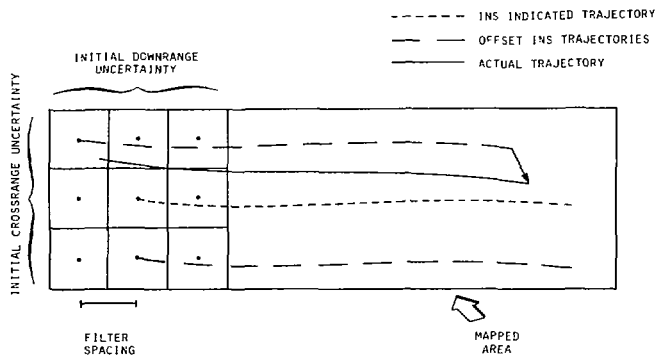

Fig. 10. Parallel filter configuration.

TABLE I
Typical AWRS Values and Final Radial Estimation Errors

Minimum AWRS Selects Filter With Minimum Estimation Error											
5.0	3.3	3.1	4.4	4.8	2.0	2111	2169	1516	1156	1108	1869
4.7	5.1	2.5	4.7	2.7	2.0	2493	1882	585	1339	395	1554
7.4	3.9	(1.1)	1.6	2.2	1.8	1556	1045	(13)	145	182	1483
2.3	3.2	2.4	2.2	2.4	2.9	412	893	122	175	1475	1504
2.1	2.6	3.9	2.5	2.6	2.6	1427	607	1073	1485	1486	1504
2.4	3.4	4.3	2.8	4.1	1.9	1758	464	764	2131	1097	2169
AWRS						Final Radial Estimation Errors (M)					

where H_i is the measurement vector containing the terrain slopes at the ith time interval, P_i is the covariance, and N is the number of measurements processed. This AWRS value is the average weighted residual squared between the predicted ground clearance for each filter and the ground clearance measured by the radar altimeter, for each time t_i. The weighting factor is inherently calculated by each Kalman filter and is simply the expected variance of Δ_i at each measurement. By examining the AWRS values for each filter after a sufficiently large number of measurements have been processed, the correct filter and its associated state error estimates can be chosen.

As an example, Table I shows AWRS values and final radial estimation errors for 36 parallel filters that were used to process a simulated test run. The test conditions were the same as before except very large initial error standard deviations of approximately 500 m were used. Each of the parallel filters utilized modified stochastic linearization and its covariance matrix was initialized with a position error standard deviation of 100 m. Note that the filter whose AWRS value is minimum also has the smallest estimation error, as desired.

It must be pointed out here, however, that if the terrain within the map is not unique, the selection algorithm might choose the wrong filter, which is the classical false fix problem. In this case, of course, the fact that there are competitive AWRS values can be detected and appropriate action taken.

Fig. 11 shows the histogram of radial misses at the target for this 36 parallel filter test case. One sees that for this

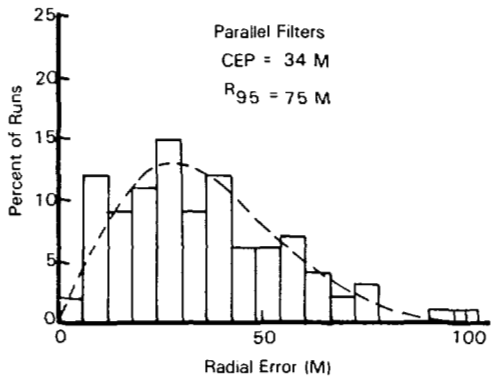

Fig. 11. Parallel filter performance.

short flight distance, the parallel filter formulation performs over on order of magnitude better than the modified stochastic linearization approach (see Fig. 9). The smoothing effect of the single-filter modified approach does not disappear until distances near 12 km, whereas each parallel filter, having been initialized with a position error standard deviation of only 100 m, can draw down much faster. This ability to converge much faster is important in some applications.

An interesting observation can be made regarding this parallel Kalman filter structure, as it can be viewed as a very general processing methodology that includes more well-known techniques as special cases. For example, at one end of the spectrum, postulate many low order filters spaced very close together. If each filter modeled only a vertical channel or measurement error bias, no terrain linearization would be required (!), and the parallel filter structure would reduce to a pure search or correlation technique such as TERCOM with a mean-square difference algorithm. On the other hand, the special case of using only one filter is the modified stochastic linearization described in Section IV. As the number of filters, associated filter spacing, and number of estimated state is varied, a spectrum of different system configuration is represented.

The final topic associated with the parallel filter approach that needs to be dealt with is the potential practical difficulty of the computational burden associated with running many Kalman filters in real time. To this end, the techniques of near optimal modeling have been used to reduce the number of modeled states, and hence simplify filter implementation [22], [23]. In that the dominant INS errors for the final application considered were position errors, three state "near optimal" filters were the basis for design. The time variation of these dominant position errors were modeled in the filters as random walks. Thus, three-state filters with driving process noise were implemented by increasing the diagonals of the position error filter covariances at each update. This technique has, of course, been used by other investigators in the design of suboptimal filters [25]. In our application, the use of three states plus process noise resulted in a 40 percent degradation in performance.

IX. Conclusions

The application of Kalman filtering techniques to the development of a terrain-aided navigation system based upon a radar altimeter sensor and a topographic reference map has been described. The fundamental difficulty in this application was the nonlinear characteristics of the terrain elevation measurement function.

Several different approaches for treating these nonlinearities were developed and limitations of each were identified. These approaches were: 1) an extended Kalman filter using local terrain slopes, 2) a quasi-linear Kalman filter based upon stochastic terrain linearization, and 3) a bank of parallel Kalman filters. This last approach led to a quite general system framework in which some commonly used terrain-aided navigation methods, e.g., TERCOM, can be interpreted as special cases.

References

[1] R. E. Kalman, "A new approach to linear filtering and prediction problems," *Trans. ASME*, vol. 82, pp. 35–45, Mar. 1960.
[2] R. E. Kalman and R. S. Bucy, "New results in linear filtering and prediction theory," *Trans. ASME*, vol. 83, pp. 95–108, Mar. 1961.
[3] R. G. Brown and D. T. Friest, "Optimization of hybrid inertial solar-tracker navigation system," in *IEEE Int. Conv. Rec.*, no. 7, 1964, pp. 121–135.
[4] S. G. Wilson, "Nonlinear filter evaluation for estimating vehicle position and velocity using satellites," *IEEE Trans. Aerosp. Electron. Syst.*, vol. AES-9, pp. 65–75, Jan. 1973.
[5] I. Y. Bar-Itzhack, "Optimal updating of INS using landmarks," in *AIAA Guidance Contr. Conf. Proc.*, Aug. 1977, pp. 492–502.
[6] W. Zimmerman, "Optimum integration of aircraft navigation systems," *IEEE Trans. Aerosp. Electron. Syst.*, vol. AES-5, pp. 737–747, Sept. 1969.
[7] J. A. D'Appolito and J. F. Kasper, Jr., "Predicted performance of an integrated OMEGA/inertial navigation system," in *Nat. Aerosp. Electron. Conf. Proc.*, May 1971, pp. 121–128.
[8] J. C. Bobick and A. E. Bryson, Jr., "Updating inertial navigation systems with VOR/DME information," in *AIAA Guidance Contr. Conf. Proc.*, Aug. 1972, paper 72-846.
[9] R. P. Moore, C. A. Hawthorne, M. C. Hoover, and E. S. Gravlin, "Position updating with microwave radiometric sensors," in *Nat. Aerosp. Electron. Conf. Proc.*, May 1976, pp. 14–19.
[10] P. G. Savage and G. L. Hartmann, "Optimum aiding of inertial navigation systems using air data," in *AIAA Guidance Contr. Conf. Proc.*, May 1976, pp. 14–19.
[11] A. J. Verderese, "Radar navigation via map matching," in *Proc. Electro-Opt. Syst. Des. Conf.*, Sept. 1972, pp. 56–62.
[12] P. J. Klass, "New guidance technique being tested," *Aviat. Week Space Technol.*, pp. 48–51, Feb. 25, 1974.
[13] W. R. Baker and R. W. Clem, "Terrain contour matching (TERCOM) primer," Tech. Rep. ASP-TR-7-61, Aeronaut. Syst. Div., Wright-Patterson AFB, OH, Aug. 1977.
[14] M. D. Mobley, "Air launched cruise missile (ALCM) navigation system development integration and test," in *Nat. Aerosp. Electron. Conf. Proc.*, May 1978, pp.1248–1254.
[15] L. D. Hostetler, "An analysis of a terrain-aided inertial navigation system," Tech. Rep. SAND75-0299, Sandia Lab., Albuquerque, NM, Sept. 1975.
[16] —, "A Kalman approach to continuous aiding of inertial navigation systems using terrain signatures," in *IEEE Milwaukee Symp. Automat. Comput. Contr. Proc.*, Apr. 1976, pp. 305–309.
[17] L. D. Hostetler and R. C. Beckmann, "The Sandia inertial terrain-aided navigation system," Tech. Rep. SAND77-7521, Sandia Lab., Albuquerque, NM, Sept. 1977.
[18] R. D. Andreas, L. D. Hostetler, and R. C. Beckmann, "Continuous Kalman updating of an inertial navigation system using terrain measurements," in *Nat. Aerosp. Electron. Conf. Proc.*, May 1978, pp. 1263–1270.
[19] L. D. Hostetler, "Optimal terrain-aided navigation systems," presented at AIAA Guidance Contr. Conf., Palo Alto, CA, Aug. 1978, and Tech. Rep. SAND78-0874, Sandia Lab., Albuquerque, NM, June 1978.
[20] L. D. Hostetler and R. C. Beckmann, "Expanding the region of convergence for SITAN through improved modeling of terrain

nonlinearities," in *Nat. Aerosp. Electron. Conf. Proc.*, May 1979, pp. 1023–1030.
[21] T. C. Sheives and R. D. Andreas, "An alternate approach for terrain-aided navigation using parallel extended Kalman filters," Tech. Rep. SAND79-2198, Sandia Nat. Lab., Albuquerque, NM, Dec. 1979.
[22] T. C. Sheives, "Reduced-order state estimation for terrain-aided navigation," Tech. Rep. SAND79-2199, Sandia Nat. Lab., Albuquerque, NM, Dec. 1979.
[23] T. C. Sheives, "State estimation using parallel extended Kalman filters on nonlinear measurements," Ph.D. dissertation, Univ. New Mexico, Albuquerque, NM, Dec. 1979, and Tech. Rep. SAND80-0013, Sandia Nat. Lab., Albuquerque, NM, Jan. 1980.
[24] A. H. Jazwinski, *Stochastic Processes and Filtering Theory*. New York: Academic, 1970.
[25] A. Gelb *et al.*, *Applied Optimal Estimation*. Cambridge, MA: M.I.T. Press, 1975.
[26] W. S. Widnall, "Enlarging the region of convergence of Kalman filters that encounter nonlinear elongation of measured range," in *AIAA Guidance Contr. Conf. Proc.*, Aug. 1972, paper 72-879.
[27] D. T. Magill, "Optimal adaptive estimation of sampled stochastic processes," *IEEE Trans. Automat. Contr.*, vol. AC-10, pp. 434–439, Oct. 1965.
[28] D. G. Lainiotis, "Optimal adaptive estimation: Structure and parameter adaptation," *IEEE Trans. Automat. Contr.*, vol. AC-15, pp. 160–170, Apr. 1971.
[29] M. Athans and C. B. Chang, "Adaptive estimation and parameter identification using multiple model estimation algorithm," Lincoln Lab. Tech. Note 1976-28, June 1976.

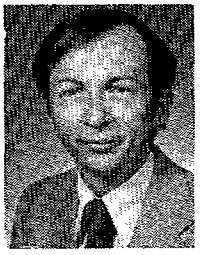

Larry D. Hostetler (S'73–M'73) was born in LaPorte, IN, on July 26, 1947. He received the B.S.E.E. degree from Purdue University, Lafayette, IN, in 1969, the M.S.E.E. degree from the Polytechnic Institute of Brooklyn, Brooklyn, NY, in 1971, and the Ph.D. degree in electrical engineering from Purdue University in 1973.

From 1969 to 1974 he was with Bell Laboratories, Whippany and Madison, NJ, where he applied statistical pattern recognition techniques to reentry vehicle discrimination. Since 1973 he has been with Sandia National Laboratories, Albuquerque, NM, and is currently Supervisor of a systems research division. His research interests include optimal estimation theory, guidance technology, and pattern recognition.

Dr. Hostetler is a member of AIAA, Eta Kappa Nu, and Tau Beta Pi.

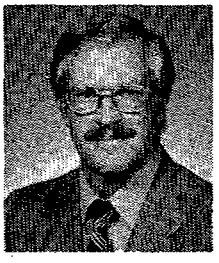

Ronald D. Andreas was born in Abilene, KS, on October 5, 1939. He received the B.S. and M.S. degrees in electrical engineering from the University of Kansas, Lawrence, in 1961 and 1963, respectively, and the Ph.D. degree in electrical engineering from the University of New Mexico, Albuquerque, in 1970.

In 1963 he joined the staff of Sandia National Laboratories, Albuquerque, NM, where he is Supervisor of an exploratory systems division. He has worked on advanced data systems, system simulation, nuclear ordinance systems, and is currently responsible for guidance and control of maneuvering reentry vehicles and Kalman aided navigation systems.

Dr. Andreas is a member of Tau Beta Pi, Eta Kappa Nu, and Sigma Xi.

Application of Multiple Model Estimation to a Recursive Terrain Height Correlation System

GREGORY L. MEALY, MEMBER, IEEE, AND WANG TANG, MEMBER, IEEE

Abstract—**This paper describes the results of an investigation of the performance capabilities of an extended Kalman filter (EKF)-based recursive terrain correlation system proposed for low-altitude helicopter navigation. The major disadvantage of this concept is its sensitivity to initial position error. One method for reducing this sensitivity involves the use of multiple model estimation techniques. In the multiple model approach, a bank of identical EKF's, each of which is initialized at a different point in the *a priori* uncertainty basket, is employed to ensure that one filter is initialized near the true aircraft position. In this manner, the probability of filter convergence is increased substantially, leading to improved navigation performance.**

Manuscript received March 3, 1982; revised September 27, 1982. This work was supported by the U.S. Army Avionics Research and Development Activity (AVRADA) under Contract DAAK80-79-C-0268.

The authors are with The Analytic Sciences Corporation, Reading, MA 01867.

0018-9286/83/0300-0323$01.00 ©1983 IEEE